

Surface Engineered Opto-electrochemical Sensing Platforms for Medical Applications



Thesis submitted in partial fulfilment
for the Award of Degree

Doctor of Philosophy

by

DIVYA

SCHOOL OF BIOCHEMICAL ENGINEERING
INDIAN INSTITUTE OF TECHNOLOGY
(BANARAS HINDU UNIVERSITY)
VARANASI – 221005
INDIA

Under the supervision of

Assoc. Prof. Pranjal Chandra
School of Biochemical Engineering

Roll No. 20011501

2025

Dedicated to my parents

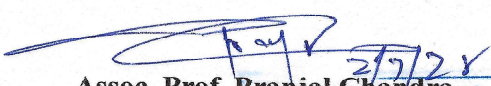
School of Biochemical Engineering
Indian Institute of Technology
(Banaras Hindu University)
Varanasi – 221005



CERTIFICATE

It is certified that the work contained in the thesis entitled “*Surface Engineered Opto-electrochemical Sensing Platforms for Medical Applications*” by “*Divya*” has been carried out under my supervision and this work has not been submitted elsewhere for a degree.

It is further certified that the student has fulfilled all the requirements of comprehensive, candidacy, and SOTA for the award of Ph.D. degree.


27/7/22
Assoc. Prof. Pranjal Chandra
(Supervisor) Dr. Pranjal Chandra
Associate Professor
School of Biochemical Engineering
School of Biochemical Engineering (BHU) Varanasi
Varanasi 221005, Uttar Pradesh
Indian Institute of Technology (BHU) Varanasi
Varanasi - Uttar Pradesh 221005, India

School of Biochemical Engineering
 Indian Institute of Technology
 (Banaras Hindu University)
 Varanasi – 221005



DECLARATION BY THE CANDIDATE

I, **Divya**, certify that the work embodied in this Ph.D. thesis is my own bonafide work and carried out by me under the supervision of **Assoc. Prof. Pranjal Chandra** from **Dec 2020 to June 2025** at the School of Biochemical Engineering, Indian Institute of Technology (BHU) Varanasi. The matter embodied in this Ph.D. thesis has not been submitted for the award of any other degree/diploma. I declare that I have faithfully acknowledged and given credit to the research workers wherever their works have been cited in my work in this thesis. I further declare that, I have not willfully copied any other's work, paragraphs, text, data, results, etc. reported in the journals, books, magazines, reports, dissertations, thesis, etc., or available at websites and have not included them in this Ph.D. thesis and have not cited as my own work.

Date: 02/07/25

Place: IIT (BHU) Varanasi

Divya
 Divya

CERTIFICATE BY THE SUPERVISOR AND HEAD OF THE DEPARTMENT

It is certified that the above statement made by the student is correct to the best of our knowledge.

Pranjal Chandra
 27/25
Assoc. Prof. Pranjal Chandra
 Supervisor Associate Professor
 School of Biochemical Engineering
 School of Biochemical Engineering
 Indian Institute of Technology (BHU)
 Varanasi - Uttar Pradesh 221005, India

Pranjal Chandra
 समन्वयक
Assoc. Prof. Pranjal Chandra
 Coordinator
 School of Biochemical Engg
 School of Biochemical Engineering
 Indian Institute of Technology
 Indian Institute of Technology (BHU)
 Varanasi - Uttar Pradesh 221005, India

School of Biochemical Engineering
Indian Institute of Technology
(Banaras Hindu University)
Varanasi – 221005



COPYRIGHT TRANSFER CERTIFICATE

Title of the Thesis: “Surface Engineered Opto-electrochemical Sensing Platforms for Medical Applications”

Name of the Student: Divya

A handwritten signature in blue ink that reads 'Divya' with a horizontal line underneath.

Copyright Transfer

The undersigned hereby assigns to the Indian Institute of Technology (BHU) Varanasi all rights under copyright that may exist in and for the above thesis submitted for the award of the Ph.D. degree.

Date: 02/07/25

Place: IIT (BHU) Varanasi

A handwritten signature in blue ink that reads 'Divya' with a horizontal line underneath.

Divya

Note: However, the author may reproduce or authorize others to reproduce material extracted verbatim from the thesis or derivative of the thesis for author's personal use provided that the source and the Institute's copyright notice are indicated.

ACKNOWLEDGEMENTS

As I write these words, I find it difficult to express the depth of my gratitude to the many individuals who have walked this journey with me. Completing this thesis has been a significant personal development journey in addition to an academic struggle. This dissertation is a testament to the collective support of all those who have impacted my life, both academically and personally.

*First and foremost, I am immensely grateful to my supervisor, **Assoc. Prof. Pranjal Chandra**, for his guidance, support, and encouragement during the journey. Thank you for the long hour discussions, continuous grilling sessions, and guidance towards completion of the tasks. I am grateful for his belief in my academic potential and ability to persevere even in my darkest hours. In uncertain times, his advice was a ray of hope.*

*I am sincerely thankful to my RPEC members **Asst. Prof. Sumit Kumar Singh**, School of Biochemical Engineering, IIT (BHU), and **Assoc. Prof. Sanjeev Kumar Mahto**, School of Biomedical Engineering, IIT (BHU), for their invaluable feedback and suggestions.*

I would like to thank all the faculty members, technical, and non-technical staff of School of Biochemical Engineering, IIT (BHU), for their cooperation and help during my work.

*Being surrounded by an encouraging and cheerful community of fellow researchers has been a huge blessing. I would like to express my heartfelt gratitude to my lab colleagues **Dr. Rahul Kumar, Dr. Shubhangi, Supratim, Rohini, Daphika, Ankur, Ratul, Dr. Indrani, Nachiket, and Aditi** for their unconditional help and support.*

Additionally, I am grateful to my friends, who offered support when it seemed hard to go on and distractions when necessary. My research experience has been enhanced by my classmates' conversations and steadfast support, which has made this journey not only feasible but also joyful.

*I would like to express my gratitude towards the **Central Instrumentation Facility Centre (CIFC), IIT (BHU) Varanasi**, for providing me instrumentation facilities.*

*I want to acknowledge the financial assistance provided by the **Ministry of Education** for providing me with the **Prime Minister Research Fellowship (PMRF)**.*

*I am also deeply thankful to **my parents** and my brothers **Sarvendra Singh** and **Dr. Manav**, because of whom I am capable of standing here and able to complete my journey. Their unwavering support and faith in my academic endeavours have been crucial to my achievement. This thesis is an expression of my family and friends' everlasting love and support throughout this difficult academic journey.*

*I would like to mention special thanks to my husband, **Abhinav**, and my **in-laws** for their love, care, and support during the most critical phase of my life. Thank you for your boundless love, patience, and understanding. I am so grateful to have you with me on this journey.*

*Finally, I am humbly grateful to the almighty **Mahadev**, without whose consent and blessings this would not have been possible.*

This thesis is not just a reflection of my work but a testament of the love, support, and kindness that has surrounded me throughout this journey.

Divya

Table of Contents

Contents	Page No.
Certificates.....	iii
Acknowledgments.....	vi
Preface.....	xxiv
 Chapter 1: General Introduction and Review of Literature	
1. Introduction	2
2. Signal Amplification of Optoelectrochemical Biosensors via Surface Engineering	4
2.1 Opto-electrochemical Biosensors	6
2.2 Nanomaterial-Based Surface Modification	8
2.3 Chemical Functionalization	16
2.4 Polymer Functionalization	21
3. Development of opto-electrochemical sensing platforms for the detection of chronic kidney disease	28
4. Different Biomarkers for Chronic Kidney Disease	31
4.1 Creatinine	32
4.2 Albumin	32
4.3 BUN (Blood Urea Nitrogen)	33
4.4 Cystatin C	34
4.5 NAG (N-Acetyl-b-D-Glucosaminidase)	35
4.6 NGAL (Neutrophil gelatinase-associated lipocalin)	35
4.7 Interleukin-18	36
5. Optical Sensors for detection of chronic kidney disease	37
5.1 Creatinine Sensor	37
5.2 Albumin Sensor	40
6. Electrochemical Sensors for detection of chronic kidney disease	51
6.1 Creatinine Sensor	51
6.2 Albumin Sensor	54
6.3 Other Biomarkers	56
7. Challenges and Possible Solutions	65
References	67

Chapter 2: Miniaturized Paper Based Optical Micro-Device for the Monitoring of Creatinine

1. Introduction	94
2. Experimental Section	97
2.1 Materials and Reagents	97
2.2 Designing of sensing probe	97
2.3 C/DZ/EDC-NHS/Anti-Cr biosensor probe testing	98
3. Results and Discussions	99
3.1 Color channel selection	99
3.2 Characterization of C/DZ/EDC-NHS/Anti-Cr/Cr probe	102
3.3 Analytical performance of C/DZ/EDC-NHS/Anti-Cr biosensor	107
3.4 Selectivity Assay	111
3.5 Real sample analysis	113
3.6 Storage, stability and reproducibility test	115
4. Device Prototyping and Deployment	115
5. Conclusion	117
References	118

Chapter 3: Hand-Held Paper Micro-Device with Integrated 3D Cascade for the Detection of Albumin in Serum Sample

1. Introduction	124
2. Experimental Section	127
2.1 Materials and Chemicals	127
2.2 Fabrication of the Reaction Zone	128
2.3 Instrumentation	129
2.4 Optical Measurements	129
3. Results and Discussions	130
3.1 Reaction Zone Characterization	130
3.2 Selection of color channel and confirmation of immunoreaction	136
3.3 Control Studies and System Validation	138
3.4 Analytical Performance	139
3.5 Interference Study	142
3.6 Analysis in Serum Sample	144
3.7 Stability and Reproducibility Test	145
4. Device Design and Fabrication	146

5. Conclusion	149
References	151
Chapter 4: Software Integrated Electrochemical Sensing Platform for the Detection of Creatinine	
1. Introduction	157
2. Experimental Section	160
2.1 Material and Methods	160
2.2 Instrumentation	161
2.3 Synthesis of boron-doped MXene (BMX)	162
2.4 Fabrication of Immunosensor	162
2.5 Electrochemical Measurements	163
3. Results and Discussions	163
3.1 Characterization of synthesized BMX	163
3.2 Surface Characterization of the fabricated sensor	166
3.3 Electrochemical characterization of the fabricated sensor	169
3.4 Analytical Performance	173
3.5 Selectivity Assay	177
3.6 Real Sample analysis	179
3.7 Repeatability and Reproducibility	180
4. Designing and Deployability of Smartphone-Integrated Sensing System	180
5. Conclusion	183
References	185
Chapter 5: Design and Development of Electrochemical Immunosensing Platform for the detection of Human Serum Albumin	
1. Introduction	191
2. Experimental Section	194
2.1 Material and Methods	194
2.2 Instrumentation	194
2.3 Preparation of the Immunosensor	195
2.4 Electrochemical Measurements	196
2.5 Real Sample Preparation	196
3. Results and Discussions	196
3.1 Physical Characterization	196
3.2 Electrochemical Characterization	201

	<i>Appendix</i>
3.3 Analytical Performance	204
3.4 Interference Study	208
3.5 Real Sample analysis	209
3.6 Repeatability and Long-term Stability	211
4. Conclusion	211
References	213
Chapter 6: Overall Summary and Future Perspective	220
Annexures	
Annexure I	225
Annexure II	244
Annexure III	246
Annexure IV	250
Biography	251

List of Figures

Figure No.	Figure Description	Page No.
Figure 1.1	Schematic representation of different types of surface engineering methods and their role in development of optoelectrochemical sensing devices	6
Figure 1.2	(a) Step-by-step fabrication of paper based optoelectrochemical sensor through coating of nanoparticles and immobilization of enzymes for the detection of paraoxon, (b) Illustration of bacterial cellulose based biosensor fabrication through incorporation of IrO ₂ nanoparticles for the detection of dopamine, (c) Schematic representation of microelectrode fabrication through electrodeposition of graphene oxide and immobilization of glucose oxidase enzyme for the detection of glucose, (d) Representation of MOF based electrochemical sensing platform immobilizing gold and aptamers for the detection of thalassemia	10
Figure 1.3	Different methods of chemical functionalization (a) EDC-NHS conjugation reaction for the immobilization of biomolecules through carboxyl group, (b) APTES-Glutaraldehyde reaction for the conjugation of biomolecules using hydroxyl group and targeting amino group, (c) Click chemistry for the conjugation of biomolecules for the signal enhancement	17
Figure 1.4	(a) Illustration of optical sensing platform using CRISP-Cas12a method and the immobilization of aptamer using EDC-NHS bioconjugation reaction, (b) Synthesis of optical platform for the	20

monitoring of the iron-regulated surface determinant protein A using the immobilization of aptamer and DNAzymes using APTES, (c) Representation of aptamer based electrochemical diagnosis of malaria biomarker lactate dehydrogenase, (j) Schematic illustration of synthesis of Co/Ni MOF and immobilization of antibody on the electrode surface using the functionalization of chemical group

- Figure 1.5** (a) Illustration of optical biosensor for the detection of aflatoxin B1 through deposition of PANI on optical fibre and using the coated fibre for the incorporation of antibodies specific to the target molecule and the analytical signal was recorded using spectrophotometer, (b) Representation of fabrication of sensing probe using the polymer deposition on electrode surface for the detection of IgG, (c) Representation of smartphone based electrochemical sensing platform for the detection of SARS CoV-2 describing the detailed fabrication method utilizing functionalization of PANI and immobilization of SARS CoV-2 specific monoclonal antibody for the detection **24**
- Figure 1.6** (a) Representation of biomarkers relating to chronic kidney disease and their clinical validation and applicability, (b) Pie-charts representing the percentage of particular sample used and the technique applied for globally developed sensors for creatinine **31**
- Figure 1.7** (a) Step-by-step representation of optical sensor developed for creatinine by dipping in the solution, (b) Showing the change in colour and signal due to presence of creatinine using the developed **40**

- sensing device, (c) Image of the developed optical device for the non-invasive detection of creatinine
- Figure 1.8** (a) Representation of sensing probe and change in intensity in presence of albumin, (b) Illustration of step-by-step fabrication process and the whole developed system for the optical detection of albumin **43**
- Figure 1.9** (a) Schematic representation of fabrication using dispenser and detection process of electrochemical sensor for creatinine, (b) Illustration of both modified and unmodified electrode for the determination of creatinine, (c) (i) Representation of modified electrode and redox mechanism (ii) Showing conversion of creatinine with enzyme and the complete reaction mechanism in solution (iii) effect of presence and absence of target molecule on signal generation **54**
- Figure 1.10** (a) Step-by-step illustration of synthesis of paper based electrochemical sensor for the albumin detection, (b) Representation of reaction occurring on electrode surface **56**
- Figure 1.11** (a) Schematic representation of step-by-step synthesis of Cystatin C specific nanobody using phage display method and layer by layer sensor designing on the surface of titanium slice, (b) Representation of modifications performed on the surface of electrode starting AuNPs deposition and further activation with primary and secondary antibody for Cystatin C detection, and the signal change **59**
- Figure 2.1** Illustration of the step-by-step fabrication of the sensor probe and the signal generation using the developed paper micro device **98**

- Figure 2.2** (a-d) Histogram showing the change in color intensity along with the real image of disc showing real-time color change, (e) Representation of change of color intensity of all the three standards through RGB analysis, i.e., Effective I_{Red} , Effective I_{Green} , and Effective I_{Blue} **101**
- Figure 2.3** (a) Histograms showing the comparative Effective I_{Blue} of the different sensing probe (i) C/DZ/EDC-NHS/Anti-Cr/Cr/PA, (ii) C/DZ/Cr/PA, (iii) C/DZ/EDC-NHS/Anti-Cr/Cr, and (iv) C/DZ/EDC-NHS/Anti-Cr/PA, (b) FTIR spectra of different stages of probe (i) C, (ii) C/DZ, (iii) C/DZ/EDC-NHS, and (iv) C/DZ/EDC-NHS/Anti-Cr **104**
- Figure 2.4** FTIR spectra of sensing probe before and after the final reaction (a) C/DZ/EDC-NHS/Anti-Cr/Cr, (b) C/DZ/EDC-NHS/Anti-Cr/Cr/PA **105**
- Figure 2.5** AFM images (a) C (z-deflection – 22.3 nm), (b) C/DZ (z-deflection – 46.8 nm), (c) C/DZ/EDC-NHS (z-deflection – 161.6 nm), (d) C/DZ/EDC-NHS/Anti-Cr (z-deflection – 199.4 nm) representing their z-deflection and micrograph. **106**
- Figure 2.6** (a) Standard calibration graph showing a linear relationship in the concentration range of Creatinine from 5 – 400 μ M, (b) Selectivity assay of C/DZ/EDC-NHS/Anti-Cr sensor probe towards interfering molecules presents in the serum and mixed sample analysis **111**
- Figure 2.7** Scatterplot showing the dose-dependent creatinine detection using the sensing probe in standard buffer and spiked serum samples **113**
- Figure 2.8** (a) Detailed design of the device setup developed for the creatinine measurement, (b) detailed dimension of the designed tunnel and the **116**

strip for image capturing and processing, (c) real image of the developed system taking reading for creatinine detection

- Figure 3.1** (a) Schematic representation of step-by-step fabrication of the reaction zone and signal generation; (b) Reaction principle and signal generation on the surface of paper micro device; (c) Real image of data analytics system using a color strip and 3-D printed device for qualitative and quantitative analysis, respectively **127**
- Figure 3.2** (a) FTIR Spectra after every modification performed on the paper surface (i) P, (ii) P/DS, (iii) P/DS/EDC-NHS, (iv) P/DS/EDC-NHS/Anti-ALB; (b) XPS survey spectra of all the modified surfaces showing the different elements present (c) S2p peaks, (d) C1s peaks, (e) N1s peaks, (f) O1s peaks **133**
- Figure 3.3** SPM Images showing 3-D surface and z-deflection of (a) P ($z = 121$ nm), (b) P/DS ($z = 223$ nm), (c) P/DS/EDC-NHS ($z = 321$ nm), (d) P/DS/EDC-NHS/Anti-ALB ($z = 427$ nm) **135**
- Figure 3.4** (a) Histogram showing the change in color intensity of RGB along with the real image of disc showing time-dependent color change, (b) Regression curve for all the three color intensities, (c) Effective I_{Red} of different control reactions: (i) P/DS/EDC-NHS/Anti-ALB/ALB/BCG, (ii) P/DS/ALB/BCG, (iii) P/DS/EDC-NHS/Anti-ALB/ALB, (iv) P/DS/EDC-NHS/Anti-ALB/BCG, (d) Standard calibration graph showing linear dynamic ranges of albumin from 1 to 60 mg/mL **137**
- Figure 3.5** (a) Selectivity assay of final paper micro-device for the tested interfering molecules and mixed-sample analysis, (b) Histogram **142**

representing the concentration-dependent ALB concentrations employing the immunosensing device in standard buffer and serum samples

- Figure 3.6** (a) Design and dimensions of all the three different pads of the developed paper micro device, (b) real images before and after ALB detection, (c) test strip developed for qualitative/semi-quantitative determination of ALB, (d) paper microdevice showing the size comparison with a five-rupee Indian coin, (e) weight of the paper device **147**
- Figure 3.7** Step-by-step process of designing of 3-D printed device with embedded light source for albumin quantification **149**
- Figure 4.1** Schematic representation of the step-by-step fabrication of immunosensor and its integration with smartphone device **160**
- Figure 4.2** (a) SEM images of synthesized Boron-doped MXene at 10 μm scale, and enlarged image at (b) 2 μm scale; (c) EDS spectrum of BMX (inset: table representing the atomic % of every element present in BMX); (d) Merged elemental mapping showing all the elements present in BMX (inset: SEM image of mapped area) (e) boron (red); (f) carbon (dark green); (g) oxygen (light green); (h) fluorine (yellow); (i) titanium (purple) distribution in the structure (Images represented at brightness +40%, contrast – 40%) **165**
- Figure 4.3** SPM 3-D images and 2-D micrograph representing z-deflection for (a) bare electrode (z-deflection: 0.97 nm), (b) AuNP layered (z-deflection: 24.7 nm), (c) AuNP/BMX (z-deflection: 75.7 nm), (d) AuNP/BMX/PANI (z-deflection: 145.4 nm), and (e) **167**

AuNP/BMX/PANI/Anti-Cret final probe (z-deflection: 209.9 nm) surfaces

- Figure 4.4** FTIR spectra of modified surfaces **(a)** BMX, **(b)** BMX/PANI, **(c)** BMX/PANI/Anti-Cret **169**
- Figure 4.5** **(a)** CV responses of bare GCE (black), GCE/AuNP (red), GCE/AuNP/BMX (blue), GCE/ AuNP/BMX/PANI (green), GCE/AuNP/BMX/PANI/Anti-Cret (purple), GCE/AuNP/BMX/PANI/Anti-Cret/Cret (yellow) modified electrode surfaces in 5 mM RuHex, **(b)** histogram representing anodic and cathodic current responses for each modified electrode surface, **(c)** EIS responses of GCE (black), GCE/AuNP (red), GCE/AuNP/BMX (blue), GCE/ AuNP/BMX/PANI (green), GCE/ AuNP/BMX/PANI/Anti-Cret (purple), GCE/AuNP/BMX/PANI/Anti-Cret/Cret (yellow) modified electrode surfaces (inset: equivalent Randles circuit; where C1, R1, and R2 represents the double layer capacitance, electrolyte resistance, and charge transfer resistance, respectively), **(d)** histogram showing the respective R_{ct} values obtained from the EIS spectra **171**
- Figure 4.6** **(a)** CV responses of the GCE/AuNP/BMX/PANI/Anti-Cret sensor probe at different scan rates (10–100 mV/s) in 5mM RuHex solution, **(b)** the corresponding linear regression for I_{pa} and I_{pc} . **173**
- Figure 4.7** **(a)** DPV responses of the GCE/AuNP/BMX/PANI/Anti-Cret sensor probe with different concentrations of creatinine (10^{-8} - 10^{-1} M) in **175**

- 5mM RuHex solution, **(b)** linear calibration curve of the response recorded with R^2 value of 0.98
- Figure 4.8** **(a)** Histogram representing the selectivity assay against interfering molecules, **(b)** Histogram representing the comparative concentrations dependent responses of creatinine in final sensing probe in buffer and serum sample **178**
- Figure 4.9** Detailed workflow representing the different stages of the software development for creatinine biosensing starting from the ideation stage to finally developed software **181**
- Figure 4.10** Screenshots of the developed software **(a)** user interface after logging the software showing ‘Test Now’ and ‘History’ options, **(b)** reading of creatinine concentration in normal clinical range represented by green mark, **(c)** reading of creatinine concentration in diseased condition represented by red mark, **(d)** user interface of the check history option representing the date, time, sample name of the test and back option to go for testing again **183**
- Figure 5.1** Illustration of step-by-step procedure for the fabrication of a final sensing probe and its deployment in the sensing of ALB in a serum sample **193**
- Figure 5.2** **(a)** SEM image of synthesized Co-MOF at 5 μm scale, **(b)** magnified image at 500 nm scale, **(c)** EDS spectrum of Co-MOF (inset: table representing the atomic % of each element) **197**
- Figure 5.3** XRD graph of **(a)** Co-MOF, **(b)** c-MWCNT, **(c)** c-MWCNT/Co-MOF with their signature peaks depicting the crystalline structure of the synthesized material **198**

- Figure 5.4** XPS spectra of (a) all the elements present in Co-MOF, MWCNT, and MWCNT/Co-MOF, (b) C1s peak, (c) N1s peak, and (d) Co2p peaks of Co-MOF (represented with green peaks as shown in complete spectra), (e) C1s and (f) O1s of MWCNT (represented with blue peaks as shown in complete spectra), (g) C1s, (h) N1s, (i) O1s, and (j) Co2p peaks of MWCNT/Co-MOF (represented with the red peaks as shown in complete spectra) **200**
- Figure 5.5** FTIR spectra of (i) Co-MOF, (ii) c-MWCNT, (iii) c-MWCNT/Co-MOF, and (iv) anti-ALB/c-MWCNT/Co-MOF **201**
- Figure 5.6** (a) CV responses of bare GCE (pink), Co-MOF/GCE (green), c-MWCNT/Co-MOF/GCE (yellow), and anti-ALB/c-MWCNT/Co-MOF/GCE (blue) electrodes in 5 mM ZS; (b) histogram showing the respective anodic and cathodic current output; (c) EIS responses of bare GCE (pink), Co-MOF/GCE (green), c-MWCNT/Co-MOF/GCE (yellow), and anti-ALB/c-MWCNT/Co-MOF/GCE (blue) electrode surfaces (inset: equivalent Randles circuit; where R1, C1, and R2 represent the solution resistance, double layer capacitance, and charge transfer resistance, respectively); (d) histogram displaying the corresponding Rct values that were derived from the Nyquist plot **203**
- Figure 5.7** (a) CV responses of the anti-ALB/c-MWCNT/Co-MOF/GCE immunosensor at varying scan rates in 5 mM ZS, (b) the corresponding linearity for anodic and cathodic peak current with a correlation coefficient (R^2) of 0.98, (c) EIS responses of the anti-ALB/c-MWCNT/Co-MOF/GCE sensor probe at different **205**

concentrations of ALB (0.1 - 60 mg/mL) in 5 mM ZS, **(d)** linear calibration curve of the response recorded with an R^2 value of 0.97

Figure 5.8 **(a)** Histogram representing the selectivity assay against interfering molecules, **(b)** Histogram depicting the final sensing probe's comparative responses in serum and buffer sample **208**

List of Tables

Table No.	Table Description	Page No.
Table 1.1	List of globally developed recent optical biosensors utilizing different surface engineering methods	13
Table 1.2	List of globally developed recent electrochemical biosensors utilizing different surface engineering methods	26
Table 1.3	List of different clinical biomarkers and their pathological ranges	34
Table 1.4	Comparison table of globally developed optical biosensors for diagnosis of chronic kidney disease	45
Table 1.5	Comparison table of globally developed electrochemical biosensors for diagnosis of chronic kidney disease	60
Table 2.1	Comparison table of some globally developed creatinine sensor with the developed set up in terms of fabrication, response time, analytical performance	109
Table 2.2	Description of the obtained Effective I_{Blue} intensity, K_{sel} of the interfering molecules	112
Table 2.3	Recovery table showing percent recoveries of creatinine in spiked serum samples and RSD values	114
Table 3.1	Representation of the % of elements presents in every modified surface obtained from XPS	131
Table 3.2	Comparison of globally developed optical ALB sensors in terms of designing, analytical performance, and clinical parameters	141
Table 3.3	Description of the obtained Effective I_{Red} intensity, K_{sel} and RSD of the interfering molecules	143

Table 3.4	Description of the recovered ALB concentrations, % recovery, and RSD using the developed sensor in serum matrix	145
Table 4.1	Comparative analysis of recently developed creatinine sensors discussing their configuration, detection technique, analytical performance, and real sample analysis	176
Table 4.2	Description of interfering molecule representing their K_{sel} and % RSD	178
Table 5.1	Representation of the % of elements presents in every modified surface obtained from XPS	199
Table 5.2	Description of the recently developed electrochemical detection of albumin comparing their fabrication and analytical details	207
Table 5.3	Description of interfering molecule along with their obtained ΔR_{ct} and their K_{sel}	209
Table 5.4	Description of the recovered ALB concentrations and % recovery using the developed sensor in serum matrix	210